Inorganic Chemistry
Article
pubs.acs.org/IC

Nitric Oxide Interaction with Oxy−Coboglobin Models Containing *trans*-Pyridine Ligand: Two Reaction Pathways

Tigran S. Kurtikyan,*[†] Shahane R. Eksuzyan,[†] John A. Goodwin,[‡] and Gohar Sh. Hovhannisyan[†]

[†]Molecule Structure Research Centre (MSRC), Scientific and Technological Centre of Organic and Pharmaceutical Chemistry NAS, 0014, Yerevan, Armenia

[‡]Department of Chemistry and Physics, Coastal Carolina University, South Carolina 29526-6054, United States

Supporting Information

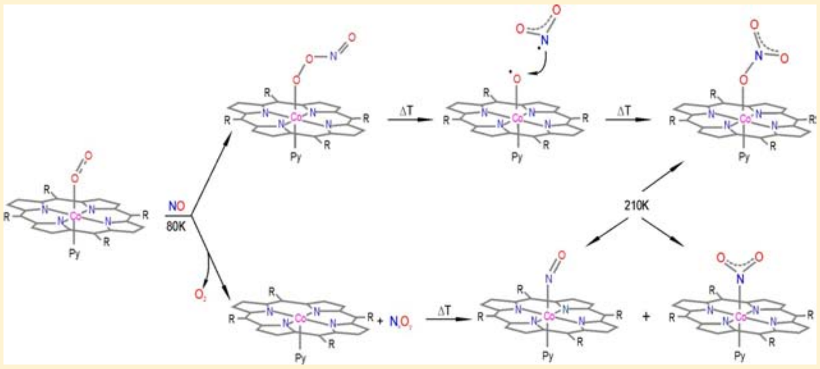

ABSTRACT: The oxy−cobolglobin models of the general formula (Py)Co(Por)(O_2) (Por = *meso*-tetraphenyl- and *meso*-tetra-*p*-tolylporphyrinato dianions) were constructed by sequential low-temperature interaction of Py and dioxygen with microporous layers of Co−porphyrins. At cryogenic temperatures small increments of NO were introduced into the cryostat and the following reactions were monitored by the FTIR and UV−visible spectroscopy during slow warming. Similar to the recently studied (NH_3)Co(Por)(O_2) system (Kurtikyan et al. *J. Am. Chem. Soc.*, **2012**, *134*, 13671−13680), this interaction leads to the nitric oxide dioxygenation reaction with the formation of thermally unstable nitrato complexes (Py)Co(Por)(η^1-ONO_2). The reaction proceeds through the formation of the six-coordinate peroxynitrite adducts (Py)Co(Por)(OONO), as was demonstrated by FTIR measurements with the use of isotopically labeled $^{18}O_2$, ^{15}NO, $N^{18}O$, and $^{15}N^{18}O$ species and DFT calculations. In contrast to the ammonia system, however, the binding of dioxygen in (Py)Co(Por)(O_2) is weaker and the second reaction pathway takes place due to autoxidation of NO by rebound O_2 that in NO excess gives N_2O_3 and N_2O_4 species adsorbed in the layer. This leads eventually to partial formation of (Py)Co(Por)(NO) and (Py)Co(Por)(NO_2) as a result of NO and NO_2 reactions with five-coordinate Co(Por)(Py) complexes that are present in the layer after the O_2 has been released. The former is thermally unstable and at room temperature passes to the five-coordinate nitrosyl complex, while the latter is a stable compound. In these experiments at 210 K, the layer consists mostly of six-coordinate nitrato complexes and some minor quantities of six-coordinate nitro and nitrosyl species. Their relative quantities depend on the experimental conditions, and the yield of nitrato species is proportional to the relative quantity of peroxynitrite intermediate. Using differently labeled nitrogen oxide isotopomers in different stages of the process the formation of the caged radical pair after homolytic disruption of the O−O bond in peroxynitrite moiety is clearly shown. The composition of the layers upon farther warming to room temperature depends on the experimental conditions. In vacuo the six-coordinate nitrato complexes decompose to give nitrate anion and oxidized cationic complex $Co^{III}(Por)(Py)_2$. In the presence of NO excess, however, the nitro−pyridine complexes (Py)Co(Por)(NO_2) are predominantly formed formally indicating the oxo-transfer reactivity of (Py)Co(Por)(η^1-ONO_2) with regard to NO. Using differently labeled nitrogen in nitric oxide and coordinated nitrate a plausible mechanism of this reaction is suggested based on the isotope distribution in the nitro complexes formed.

INTRODUCTION

Although nitric oxide (NO) plays important regulatory functions in mammalian biology,[1,2] its overproduction is harmful mainly due to reaction with superoxide anion, leading to formation of the peroxynitrite anion, a powerful oxidizing and nitrating agent.[3] It is commonly accepted that heme proteins are the principal agents responsible for the NO scavenging.[4] The main part for NO scavenging involves its direct reaction with HbO_2 (Hb = hemoglobin) in red blood cells, leading to formation of the nitrate anion and the ferric form of the protein, metHb. It is suggested that this process

Received: July 19, 2013
Published: October 3, 2013

proceeds through the formation of coordinated peroxynitrite, which undergoes homolytic O−O bond cleavage, forming oxo−ferryl species and free radical nitrogen dioxide NO_2. The NO_2 nitrogen attacks the ferryl Hb oxo ligand, and the O-bound nitrate is formed, the decay of which results in metHb and nitrate anion.[4] However, until now the unequivocal experimental evidence confirming the formation of coordinated peroxynitrite at the initial stage of the nitric oxide dioxygenation (NOD) reaction has been obtained neither for heme-containing globins nor for modeling iron−porphyrins.[5−7] Moreover, the recent time-resolved UV−vis spectroscopy experiments by Pacheco and coauthors[8] on (oxy)Mb (Mb = myoglobin) also call into question the formation of a (ferryl)Hb and NO_2 caged pair in the course of the NOD reaction.

A few years ago a spectroscopic study was carried out in our laboratory to probe the viability of a $Fe^{III}(OONO)$ intermediate in the reaction of the six-coordinate oxy−heme model complex $(NH_3)Fe(Por)(O_2)$ (Por = *meso*-tetraphenyl- and *meso*-tetra-*p*-tolylporphyrinato dianions) with NO in low-temperature sublimed solids.[7] Surprisingly, at temperatures as low as 80−100 K the six-coordinate nitrato complexes $(NH_3)Fe(Por)(\eta^1\text{-}ONO_2)$ were formed without spectral detection of any intermediates. In particular, peroxynitrite complexes were not observed, and this result implied that, if formed, isomerization of this putative intermediate to the nitrato product was quite facile, even under these conditions.

It was shown recently that the oxy−coboglobin modeling compound $(NH_3)Co(Por)(O_2)$ also promotes the NOD reaction.[9] In this case the formation of six-coordinate nitrato complexes begins at 180 K, and at lower temperatures, the intermediates were spectrally detected, throwing light on the mechanism of this biologically important transformation. It was demonstrated that the sequence of the reactions followed the stages suggested for heme proteins,[4] particularly the formation of the coordinated peroxynitrite which was proposed based on the FTIR spectral data with use of labeled $^{18}O_2$, ^{15}NO, and $N^{18}O$ and DFT calculations. It should be mentioned here that, although as valuable as model compounds Co−porphyrins are, they cannot be considered equal with heme systems. For example, Co promotes/stabilizes the superoxo character of the corresponding dioxygen adducts to a much higher extent than Fe, Co(III) has a higher preference toward six-coordination than Fe(III), Co(III) is more kinetically inert than Fe(III), etc.[10] All this can lead to different mechanisms and characteristics of intermediate species along reaction pathways, and the observed intermediates are more related to the chemistry of cobalamins and their interactions with nitrogen oxides species.

In this study the reaction of nitric oxide (NO) with specially constructed porous layered solids of the oxy−coboglobin models containing the *trans*-pyridine ligand $(Py)Co(Por)(O_2)$ was monitored by FTIR and UV−visible spectroscopy from 80 K to room temperature. We used the sublimed layers methodology,[11] which is based on the preparation of the porous layered solids by the vacuum sublimation of metal *meso*-tetraarylporphyrinato complexes onto a substrate cooled by liquid nitrogen (LN_2). The facile reactions of these oxy−coboglobin models with volatile reactants can be monitored by FTIR and optical spectroscopy over a wide temperature range without the masking effects of solvents.

As expected, the NOD reaction proceeds also with these coboglobin models to give thermally unstable six-coordinate nitrato complexes $(Py)Co(Por)(\eta^1\text{-}ONO_2)$. In $(Py)Co(Por)(O_2)$, however, the Co−O_2 bond is weaker and some O_2 is released (eq 1), resulting partly in NO autoxidation (eq 2):

$$(Py)Co(Por)(O_2) \leftrightarrow (Py)Co(Por) + O_2 \quad (1)$$

$$2NO + O_2 \rightarrow 2NO_2 \quad (2)$$

Under low-temperature conditions, the NO_2 formed in this way reacts with excess NO or another NO_2 molecule to give *asym*-N_2O_3 (eq 3) and *sym*-N_2O_4 (eq 4)

$$NO_2 + NO \leftrightarrow asym\text{-}N_2O_3 \quad (3)$$

$$NO_2 + NO_2 \leftrightarrow sym\text{-}N_2O_4 \quad (4)$$

as the more stable forms of dinitrogen trioxide and dinitrogen tetroxide correspondingly, formation of which may be easily monitored by FTIR measurements. This leads eventually to partial formation of (Py)Co(Por)(NO) and $(Py)Co(Por)(NO_2)$ as a result of NO and NO_2 reactions with five-coordinate Co(Por)(Py) (eqs 5 and 6):

$$(Py)Co(Por) + NO \rightarrow (Py)Co(Por)(NO) \quad (5)$$

$$(Py)Co(Por) + NO_2 \rightarrow (Py)Co(Por)(NO_2) \quad (6)$$

The intermediates preceding the formation of the main products of the reaction six-coordinate nitrato complexes $(Py)Co(Por)(\eta^1\text{-}ONO_2)$ were detected by FTIR spectroscopy with the use of experiments with isotopically labeled $^{18}O_2$, ^{15}NO, $N^{18}O$, and $^{15}N^{18}O$ species. On the basis of these spectral data and DFT calculations, the formation of coordinated peroxynitrite at the initial stage of NOD reaction is proposed. The presence of some NO autoxidation products in the layers gave an opportunity to prove the existence of the caged radical pair after homolytic O−O bond cleavage in the coordinated peroxynitrite moiety. It has been also shown that in NO atmosphere the nitrate complexes $(Py)Co(Por)(\eta^1\text{-}ONO_2)$ pass to the nitro species $(Py)Co(Por)(NO_2)$, formally indicating the oxo-transfer reactivity of six-coordinate nitrato complexes with regard to NO.

■ EXPERIMENTAL SECTION

Co(TPP) and Co(TTP) were synthesized using the literature methods.[12] Before sublimation they were additionally purified by column chromatography with dry alumina using reagent grade chloroform as the eluent. NO (^{15}NO, $N^{18}O$, $^{15}N^{18}O$) was purified by passing it through KOH pellets and a cold trap (dry ice/acetone) to remove the higher nitrogen oxides and trace quantities of water. The purity was checked by IR measurements of the layer obtained by slow deposition of NO onto the cold substrate of the optical cryostat (77 K). The IR spectrum did not show the presence of N_2O, N_2O_3, or H_2O. ^{15}NO with 98.5% enrichment was purchased from the Institute of Isotopes, Republic of Georgia, and was purified by the same procedures. $N^{18}O$ and $^{15}N^{18}O$ were obtained by the reduction of $N^{18}O_2$ ($^{15}N^{18}O_2$) over metallic Hg in an evacuated flask. $N^{18}O_2$ and $^{15}N^{18}O_2$ were synthesized according to the following procedure. The 1:2 mixture of N_2($^{15}N_2$) and $^{18}O_2$ gases (Cambridge Isotopic Laboratories) was introduced into an evacuated glass balloon provided with inserted electrodes. Upon continuous electric discharge the colorless gas mixture turned reddish-brown, indicating the formation of $N^{18}O_2$ ($^{15}N^{18}O_2$). Pyridine and deuterated pyridine (Py-d_5, Aldrich) were distilled under sodium before use.

Sublimed layers of Co(TPP) [Co(TTP)] were obtained on the cold (77 K) KBr support of an optical cryostat according to the published procedure.[11] Then about 0.3 Torr equivalent of Py was added at LN_2 and the layer was annealed at 160−170 K, temperatures at which the formation of Co(Por)(Py) was completed. A few tenths Torr of O_2 was then introduced into the cryostat at LN_2 and annealed to assist in

Scheme 1

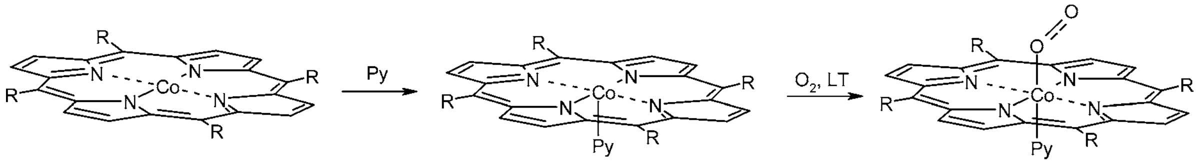

R - phenyl, p - tolyl

the formation of the desired mixed dioxygen complexes (Py)Co(Por)(O_2). Both of these processes can be controlled while monitoring by FTIR spectroscopy according to the shifts of some of the porphyrin bands. After obtaining the desired six-coordinate dioxygen complexes, the cryostat was pumped out at 90 K, and then the layer was cooled by LN_2 and a small increment (~0.4 Torr equivalent) of NO was introduced into the cryostat. The layer was then slowly warmed to room temperature, and the FTIR or UV–visible spectra were obtained at various controlled temperatures measured by a thermocouple. The UV–visible spectra were taken after the FTIR measurements of the same samples confirmed the identity of each species. The FTIR and UV–visible spectra were acquired on a Nexus (Thermo Nicolet Corp.) in the spectral range 400–4000 cm^{-1} with a resolution of 2 cm^{-1} and a Specord M-40 (Carl Zeiss, Jena) or Helios γ (Thermo Electron Corp.) spectrometer in the range of 350–900 nm, respectively.

Computational analysis was carried out with Spartan ’10 software (Wave function, Inc.) running under a Windows operating system. Equilibrium geometries for the low-spin, ground-state derivatives of (Py)Co(P)(OONO) (P = porphinato dianion) were first determined by DFT (BP/6-31G*) methods and IR frequencies calculated from the resulting structures. In the case of the cis forms of (Py)Co(P)(OONO) and (Py)Co(TPP)(OONO), the OONO dihedral angle was locked at 0.0° in the determination of the equilibrium geometry and IR spectrum. The relative energies of the cis and trans isomers were determined from the Spartan ’10 thermodynamics program based upon geometries determined by DFT methods and IR frequencies determined by DFT methods for the (Py)Co(P)(OONO) models. Likewise, DFT methods were used with Spartan ’10 for determining equilibrium geometries, IR frequencies, and thermodynamics parameters for the cis and trans (OONO) isomers of (Py)Co(TPP)(OONO).

■ RESULTS AND DISCUSSION

Construction of Six-Coordinate Oxy–Coboglobin Models. To construct the six-coordinated dioxygen complexes of porphyrins with *trans*-pyridine ligand (Py)Co(Por)(O_2), the strategy demonstrated in Scheme 1 was applied. In contrast to iron–porphyrins, the first axial ligand binding constant K_1 in Co–porphyrins is much greater than that of the second ligand K_2.[13] This allows one to obtain the five-coordinate complexes of (Py)Co(Por) by the reaction of small quantities of Py with amorphous layers of Co–porphyrins. As monitored by a vacuum gauge, low pressures of Py (~0.3 Torr equivalent) were supplied into the cryostat at low temperatures, and the layers were allowed to be warmed until ~170 K, where the formation of five-coordinated complexes was completed.

FTIR spectra served as a reliable tool for monitoring this process, since some porphyrin bands underwent noticeable shifts upon the Co(Por) + Py → Co(Por)(Py) transition. An example of the spectral changes observed upon formation of Co(Por)(Py) complexes is reproduced in Figure S1a,b (Supporting Information). Intense porphyrin bands of Co(TPP) in the vicinity of 1000 cm^{-1} shift to lower frequencies and change their relative intensities. The same occurs with the single porphyrin band of Co(TTP) in this spectral range. Notably, when six-coordinated dioxygen complexes (Py)Co(Por)(O_2) were formed upon exposition of this species under O_2 at low temperatures, these bands shifted back to their initial positions (Figure 1). It is reasonable to suggest that these spectral changes upon Py binding are connected with the out-of-plane motion of the Co center in the five-coordinate complex, followed by a shift back of the Co center into the plane of the porphyrin when O_2 binds. Such out-of-plane motion perturbs the overlapping between metal d_π-orbitals and porphyrin e_g*-orbitals, resulting in changes of energy of some porphyrin vibrations.

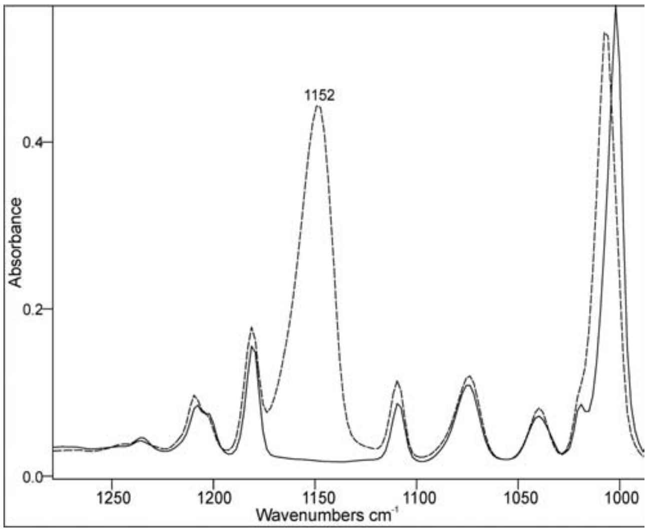

Figure 1. FTIR spectra of thin layers Co(TTP)(Py-d_5) (solid line) and Co(TTP)(Py-d_5)(O_2) (dashed line), T = 80 K.

After the formation of the five-coordinate pyridine complexes, Co(Por)(Py), a few tenths Torr of O_2($^{18}O_2$) was supplied into the cryostat at LN_2 temperature, and the layer was allowed to warm under O_2 atmosphere to ~160 K, at which temperature the intensity of the $\nu(O_2)$ band which characterizes the dioxygen complex (Py)Co(Por)(O_2) reached maximum intensity. The layer was then cooled to LN_2 temperature and the O_2 excess was pumped out. The pumping was continued upon layer warming to about 90 K to try to eliminate the traces of O_2 adsorbed in the layer. At higher temperatures long-term pumping leads to the gradual elimination of the coordinated O_2 as is seen from the decreasing intensity of the $\nu(O_2)$ band. This observation is in contrast with the previously studied six-coordinate dioxygen adducts with ammonia, (NH_3)Co(Por)(O_2), for which the pumping at 120 K allowed the complex to remain intact.[9] Hence the dioxygen binding in the pyridine derivative is weaker than for the ammonia complex, which is also reflected in the value of $\nu(O_2)$ (see below).

The IR spectra of six-coordinate adducts (Py)Co(Por)(O_2) in the range of dioxygen stretching reveal an intrinsic complexity caused by vibrational coupling with coincidentally degenerate porphyrin and pyridine modes. As an example, the FTIR spectra of (Py)Co(TPP)(O_2) and (Py-d_5)Co(TPP)(O_2) are represented in the Supporting Information (Figure S2). This behavior is similar to that observed in the resonance Raman spectra (RRS) of analogous systems.[14] The detailed analysis of FTIR spectra of the (Py)Co(Por)(O_2) species will be presented elsewhere. Here we briefly mention that if the energy of the O_2 stretching closely matches the energies of the vibrational modes of the porphyrin, the *trans*-pyridine ligand, as well as the pyridine molecules that are in direct contact with the coordinated O_2, the intensities of the latter bands are enhanced by the vibrational coupling with $\nu(O_2)$ stretching. As a result, numerous new bands rise in this spectral range and the isotope shifts upon using $^{18}O_2$ are not ideal.

In our study we used also deuterated pyridine-D_5 that, in contrast to pyridine-H_5, leaves some important spectral ranges band-free. Notably, it does not have the IR bands in the range of $\nu(O_2)$. With this and Co(TTP) as a porphyrin, we were able to obtain the FTIR spectra in the $\nu(O_2)$ range with a single band of coordinated dioxygen not perturbed by vibrational coupling with pyridine and porphyrin modes lying in the same spectral range. This was important for the reliable estimation of the $\nu(O_2)$ value.

Figure 1 demonstrates the spectral changes upon the reaction of O_2 with Co(TTP)(Py-d_5). The intense band at 1152 cm^{-1} that appeared in the spectrum is shifted to 1089 cm^{-1} by $^{16}O_2/^{18}O_2$ substitution. Therefore, this band must be assigned to $\nu(O_2)$ of the respective dioxygen adducts. The observed isotope shift (63 cm^{-1}) is very close to that expected for a harmonic diatomic oscillator (65 cm^{-1}). These results indicate the formation of six-coordinate dioxygen complexes, since the $\nu(O_2)$ in five-coordinate complexes with Co(TPP) appears at 1278 cm^{-1} in an Ar matrix[15] and 1251 cm^{-1} in sublimed layers.[16] The absence of the $\nu(O_2)$ band in the 1250 cm^{-1} range (Figure 1) also indicates that there are no unligated Co—porphyrin molecules in the layer. Formation of the six-coordinate dioxygen complexes is also supported by the changes in the UV—visible spectra (Figure 2 for TPP derivative) that manifest the formation of six-coordinate dioxygen complexes with the trans electron donor ligand.[17]

Systematic RRS studies of the effect of axial ligand basicity on the frequency of ν(O—O) in O_2 adducts of cobalt porphyrin complexes with a large number of pyridine derivatives revealed the linear relationship between pK_a of *trans*-pyridine ligand and ν(O—O).[14a] Higher basicity of the trans ligand leads to a lower $\nu(O_2)$ due to additional electron density on the π^* antibonding molecular orbital of dioxygen. Although direct comparison between NH_3 and Py ligands is inappropriate, since the latter is also a π-acceptor ligand while the former is a saturated system, it seems that the same pattern is operational here, too. The $\nu(O_2)$ stretching frequency of the six-coordinate complex with *trans*-ammonia (NH_3)Co(TPP)(O_2) is disposed at 1139 cm^{-1}, which is noticeably lower than for pyridine ligand. Taking into account the higher basicity of NH_3 (pK_a = 10.5) relative to Py (pK_a = 5.25), this is the expected result. The lower frequency of O_2 stretching mode indicates stronger binding of dioxygen with the metal,[14b] so in the six-coordinate ammonia derivative the O_2 is bound more strongly than in the case of analogous complexes with the pyridine ligand, which is also evident from their relative stabilities (see above).

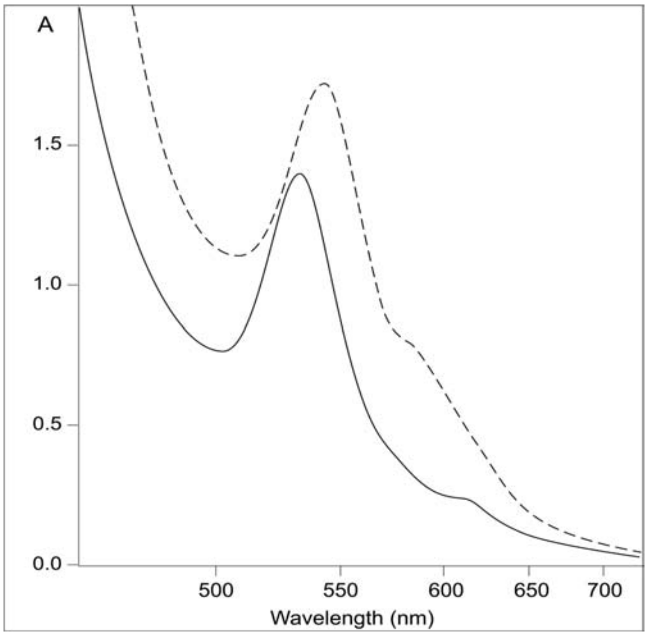

Figure 2. UV—visible spectra of layered Co(TPP) (solid) and (Py)Co(TPP)(O_2) (dashed) (T = 80 K). The dashed spectrum was taken after FTIR measurements of the same sample confirmed the formation of six-coordinate dioxygen complex.

Reaction of NO with Six-Coordinate Dioxygen Complexes. After constructing the six-coordinate dioxygen complexes, (Py)Co(Por)(O_2), the small increment (~0.4 Torr equivalent) of previously cooled NO was introduced into the cryostat, and its low-temperature interaction with oxy—coboglobin modeling compound was spectrally monitored upon slow warming of the layers. It is necessary to note that for the spectral characterization of intermediates formed at this stage of reaction the FTIR spectrum of Co(TTP) is more convenient compared to Co(TPP). Particularly, the band connected with the ring stretching vibration of tolyl groups in the vicinity of 1600 cm^{-1} has a very low intensity, and the interval between 700 and 800 cm^{-1} is relatively free of bands compared to the TPP derivative. Additionally Py-d_5 leaves free the 1600 cm^{-1} range where natural pyridine has intense absorption. The spectral changes observed upon the reaction of NO with layered (Py)Co(TTP)(O_2) are demonstrated in Figure 3. The band of coordinated dioxygen in the 1150 cm^{-1} range, which acts in the form of a doublet, decreases in intensity, and a set of new bands denoted by arrows grow with correlating intensities in the vicinity of 1600, 950, 740, and 540 cm^{-1}, which belong to an intermediate that is fairly stable until 140 K but after further warming begins to decompose. These bands had their analogs when $^{18}O_2$, ^{15}NO, N^{18}O, and ^{15}N^{18}O isotopomers were used in the experiments. These data are summarized in Table S1 (Supporting Information), together with calculated values of stretching frequencies and their isotopic shifts, and assume the formation of the O-coordinated peroxynitrite (Scheme 2), as it was observed for analogous experiments with ammonia derivative (NH_3)Co(TTP)(O_2).[9]

For the pyridine derivative, however, together with the bands of coordinated peroxynitrite, a number of new bands also grow that in Figure 3 are denoted by one and two asterisks. These bands are disposed at 1835, 1732, ~1600, 1294, 1255, and ~770 cm^{-1} and have their isotopic counterparts at 1805, 1699,

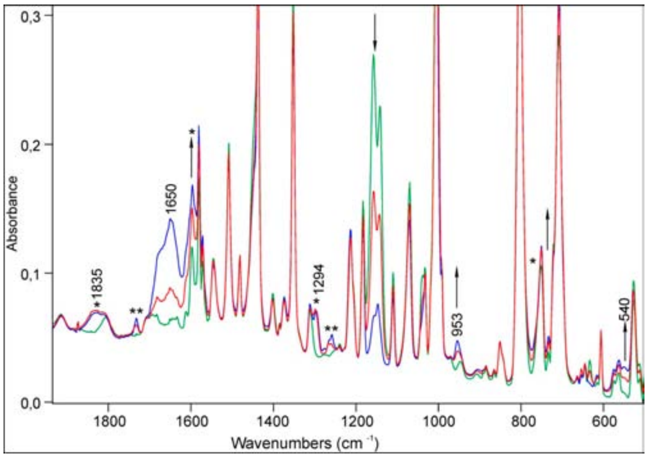

Figure 3. FTIR spectral changes accompanying formation of (Py)Co(TTP)(OONO) after addition of small quantities of NO on the layered (Py)Co(TTP)(O_2) upon warming from 80 to 130 K. The bands denoted by arrows is that of coordinated peroxynitrite moiety. The bands denoted by * belong to *asym*-N_2O_3 and those by ** to sym-N_2O_4.

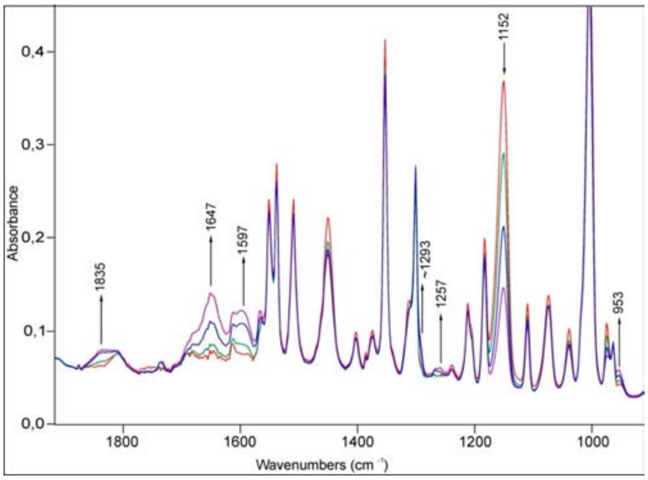

Figure 4. FTIR spectral changes after addition of NO (~0.4 Torr equivalent) to the layer containing (Py-d_5)Co(TTP)(O_2) and slow warming from 80 to 140 K.

~1570, 1277, and ~760 cm^{-1} when ^{15}NO is used in the experiments.

The bands disposed at 1835 (1805), ~1600 (~1570), 1294 (1277), and ~770 (~760) cm^{-1} certainly belong to the $\nu(NO)$, $\nu_a(NO_2)$, $\nu_s(NO_2)$, and $\delta(NO_2)$ modes of the relatively stable form of dinitrogen trioxide *asym*-N_2O_3,[18] while those at 1732 (1699) and 1255 (1245) cm^{-1} indicate the presence of dinitrogen tetroxide *sym*-N_2O_4.[19] It is necessary to note that the N=O stretching of coordinated peroxynitrite[9] is occasionally disposed in the same spectral range (~1600 cm^{-1}) as the $\nu_a(NO_2)$ mode of N_2O_3 and increases its intensity. As showed in separate experiments with N_2O_3 adsorbed in the amorphous Ni(TPP) layer,[20] the intensity of the high-frequency $\nu(NO)$ and $\nu_a(NO_2)$ bands of this species are about equal, while in the experiments with Py-d_5, for which pyridine bands in this range are shifted to lower frequencies, the band at ~1600 cm^{-1} (Figure 4) is much more intense than the band at 1835 cm^{-1}, implying the overlapping of two bands in the 1600 cm^{-1} spectral range.

These data indicate that a small quantity of bound O_2 is released, leading to the partial oxidation of NO adsorbed in the layer (eq 2, Scheme 3). Oxidation of NO by O_2 is a classic example of an elementary trimolecular reaction, but its mechanism still the subject of intense experimental and theoretical studies.[21] Regarding our low-temperature study, we were not able to detect any intermediates preceding the formation of *asym*-N_2O_3 and *sym*-N_2O_4.

In the spectra given in Figures 3 and 4, there is another growing band at ~1650 cm^{-1} that in experiments with ^{15}NO appears at ~1620 cm^{-1}. This band should be assigned to six-coordinate nitrosyl complex (Py)Co(TTP)(NO)[22] formed upon NO interaction with (Py)Co(TTP) after release of coordinated O_2. These six-coordinate nitrosyl species are stable at low temperatures and decompose to give well-known five-coodinate nitrosyl complexes Co(Por)(NO) upon warming to room temperature.[22]

The intensity ratio of the bands belonging to coordinated peroxynitrite and oxidation products N_xO_y depends on the experimental conditions. It was noticed that an excess of Py in the layer gives preference to the formation of the peroxynitrite intermediate, which might be expected since NO oxidation requiring the collision of three molecules (2NO + O_2)[21d] should be difficult in Py matrices due to the reduced diffusion rate in this conditions.

Thyagarajan and co-workers attempted to isolate a peroxynitrito complex from the reaction of the dioxygen complex of tris(pyrazolyl)boratecobalt^{II} [$Tp^{t\text{-}Bu,Me}Co(O_2)$] with an excess of NO in tetrahydrofuran solution.[23] At temperatures below −61 °C an intermediate was observed with the bands at 1849, 1598, and 1301 cm^{-1}. The first of them was assigned to dissolved NO, while two others may have been the bands of desired peroxynitrito complex. Taking into account the result of a recent paper[9] containing information about the FTIR spectral manifestation of (NH_3)Co(Por)(OONO) and the data obtained in this work, we are prone to think that the bands reported in that work[23] more likely belong to N_2O_3. Remarkably, this reaction yielded the nitrato $Tp^{t\text{-}Bu,Me}Co(NO_3)$ and nitro $Tp^{t\text{-}Bu,Me}Co(NO_2)$ complexes, the result closely related to that in this paper.

Decomposition of the Peroxynitrite Intermediate. Evidence of Caged Radical Pair Formation. Warming the layer from 150 to 170 K leads to the disappearance of bands belonging to the peroxynitrite intermediate, while those of N_2O_3 and N_2O_4 remains intact, even after pumping at 150 K. It

Scheme 2

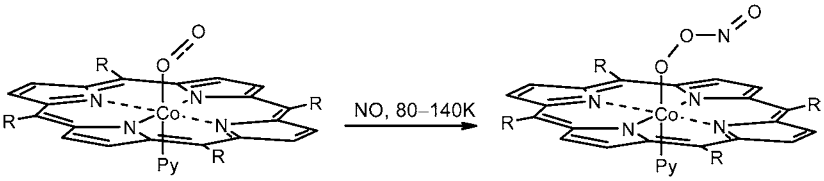

Scheme 3

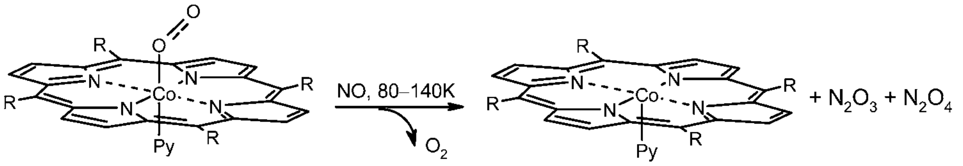

was suggested for the analogous system with *trans*-ammonia ligand that disruption of the O−O bond in peroxynitrite moiety leads to the formation of a caged radical pair consisting from NO_2 and $(NH_3)(Por)Co{=}O \leftrightarrow (NH_3)(Por)Co{-}O^{\bullet}$.[9] In that study there was FTIR spectral evidence for formation of NO_2, but the cobaltyl species was not identified. According to DFT calculations the $\nu(Co{=}O)$ vibration should appear at 691 cm^{-1}, and at 660 cm^{-1} for ^{18}O-labeled analog. However, an isotopically sensitive band in this spectral range was not found. It probably had a very low intensity and was obscured by the bands of the porphyrin itself. This species was not observed in pyridine derivatives either, for which DFT calculations give values of 676 (646) cm^{-1}. Additionally, the spectral detection of NO_2 in the presence of above-mentioned oxidized species is complicated, since their bands are disposed in close proximity to each other. However, for the pyridine derivative studied in this work, the presence of some *asym*-N_2O_3 in the layer gave a nice opportunity to confirm the formation of a caged radical pair after cleavage of O−O bond in peroxynitrite moiety using differently labeled nitric oxide in the different stages of the reaction.

Initially, the interaction of labeled ^{15}NO with (Py)Co(Por)-(O_2) (experiment a) was carried out and the layer was warmed to 170 K. At this temperature the FTIR spectrum of the layer reveals the presence of labeled $^{15}N_2O_3$ and $^{15}N_2O_4$ and complete disruption of the O−O bond of coordinated peroxynitrite. Then the temperature was lowered to 150 K, the excess of ^{15}NO was pumped out, and a portion of natural abundance NO was introduced into the cryostat. FTIR spectra of this system were measured at various temperatures upon slow warming. As has been demonstrated earlier[20] and is shown here, beginning from 140 K the isotope exchange reaction occurs, and at 170 K all the $^{15}N_2O_3$ passes to N_2O_3, as is obvious from the high frequency shifts of the 1805 and 1277 cm^{-1} bands to 1835 and 1294 cm^{-1} (Figure S3, Supporting Information).

Further slow warming of the system from 180 to 210 K leads to the spectral changes represented in Figure 5a. The $\nu_s(NO_2)$ band of N_2O_3 at 1294 cm^{-1} decreases in intensity, and a number of new bands grow in intensity. Marked by an arrow is the low-frequency shoulder of the intense band in the vicinity of 1440 cm^{-1}, which consists of the overlapping bands of the porphyrin and the Py excess still present in the layer, and the band at 1311 cm^{-1}, which should be assigned to the $\nu_a(NO_2)$ and $\nu_s(NO_2)$ of the six-coordinate nitro complexes (Py)Co-(TPP)(NO_2).[22b] Confirming this assignment, the band with correlating intensity that grows at 816 cm^{-1} represents the $\delta(NO_2)$ vibration in this compound (Figure S4a, Supporting Information).

The band in the high-frequency range of the combined band at ∼1440 cm^{-1} and those at 1249 and ∼975 cm^{-1} (shown in the Figure S4a, Supporting Information) should be assigned to the $\nu_a(^{15}NO_2)$, $\nu_s(^{15}NO_2)$, and $\nu(O{-}^{15}N)$ of the six-coordinate nitrato complex with labeled nitrogen (Py)Co(TPP)(η^1-$O^{15}NO_2$) (see below). The band at 1271 cm^{-1} represents the $\nu_s(NO_2)$ of (Py)Co(TPP)(η^1-ONO_2) with the natural nitrogen. The quantity of this species is about 15% with respect to the labeled complex, assuming the closeness of the extinction coefficient of labeled and natural compounds. Hence, surprisingly the nitro complex contains natural nitrogen while in the nitrato complex the nitrogen is labeled.

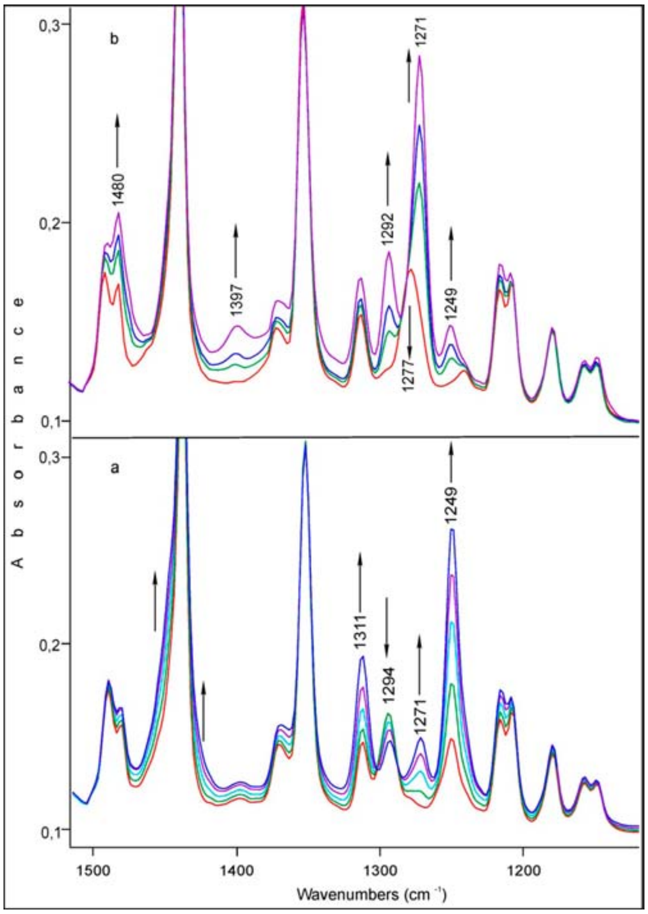

Figure 5. FTIR spectral changes upon warming from 180 to 210 K the layers of (Py)Co(TPP)(O_2) + ^{15}NO system (a) under 3 Torr NO and (Py)Co(TPP)(O_2) + NO system (b) under 3 Torr ^{15}NO. For experimental details, see the text.

An analogous experiment was carried out, in which the NO and ^{15}NO gases were supplied in reverse order (experiment b). Initially NO was introduced into the cryostat at 80 K and the layer was warmed to 170 K. At this temperature the FTIR spectrum of the layer reveals the presence of N_2O_3 and N_2O_4 and complete disruption of the O−O bond of the coordinated peroxynitrite. The layer was cooled to 150 K, the excess NO was pumped out, and a portion of ^{15}NO was supplied into the cryostat. Upon warming the layer to 170 K the bands of N_2O_3 at 1835 and 1294 cm^{-1} shift to 1805 and 1277 cm^{-1}, showing complete isotope exchange and the formation of $^{15}N_2O_3$. Further warming of the layers from 180 to 210 K is accompanied with the spectral changes represented in Figure 5b. Two sets of bands grow in intensity at 1397, 1292, and 808 cm^{-1}, and 1482, 1271, and ~985 cm^{-1} (the low-frequency bands are demonstrated in Figure S4b, Supporting Information). The first set should be assigned to $\nu_a(^{15}NO_2)$, $\nu_s(^{15}NO_2)$, and $\delta(^{15}NO_2)$ of $(Py)Co(TPP)(^{15}NO_2)$,[22b] while the bands of the second set consist of the $\nu_a(NO_2)$, $\nu_s(NO_2)$, and ν(O−N) stretching of nitrato complex (Py)Co(TPP)(η^1-ONO_2) (see below). Hence, the nitro complex contains the labeled $^{15}NO_2$, while nitrato complex is not labeled. A small band at 1249 cm^{-1} is that of the $\nu_s(^{15}NO_2)$ stretching of the labeled nitrato complex (Py)Co(TPP)(η^1-$O^{15}NO_2$).

These data can be interpreted unequivocally by assuming that after disruption of the peroxynitrite O−O bond the caged radical pairs consisting of (Py)(Por)Co−O$^\bullet$ and $^{15}NO_2$ (experiment a) and (Py)(Por)Co−O$^\bullet$ and NO_2 (experiment b) are formed. For experiment a, being in the radical cage, the $^{15}NO_2$ molecule does not react with NO to form different isomeric forms of dinitrogen trioxide[18] to undergo isotope exchange. With this assumption it is possible to explain why under the reaction conditions N_2O_3 dissociates to give NO and NO_2, as indicated by the formation of (Py)Co(TPP)(NO_2), and only a minor quantity of the six-coordinate nitrato complex with unlabeled nitrato group is formed. It means that at 180−210 K temperature range only a small part of $^{15}NO_2$ escapes the radical cage. The same arguments can be given when interpreting the results of experiment b.

Formation of Six-Coordinate Nitrato Complexes (Py)Co(Por)(η^1-ONO_2) and Their Decomposition upon Warming to Room Temperature. Further slow warming of the layer from 180 to 210 K leads to growth of three new bands in the vicinity of 1480, 1270, and 985 cm^{-1} (Figure 6). These bands have their isotopic counterparts at ~1450, 1250, and 970 cm^{-1} when ^{15}NO was used and at 1422, 1210, and 931 cm^{-1} when $^{15}N^{18}O$ and $^{18}O_2$ were used in the experiments (Figure 7). The frequencies of the new species formed in the 180−210 K temperature interval in the experiments with the natural abundance O_2 and NO and different ^{18}O- and ^{15}N-containing isotopomers with their various combinations are summarized in Table 1. The positions of these bands and their relative intensities and isotopic shifts are close to those observed in the six-coordinate nitrato complexes of iron−porphyrins obtained by the low-temperature interaction of electron-donor ligands[24] with bidentate nitrato complexes Fe(Por)(η^2-O_2NO)[25] as well as by the NOD reaction mediated by oxy Fe− and Co−porphyrins containing *trans*-ammonia ligand[7,9] and can be unambiguously assigned to the six-coordinate nitrato complexes (Py)Co(Por)(η^1-ONO_2).

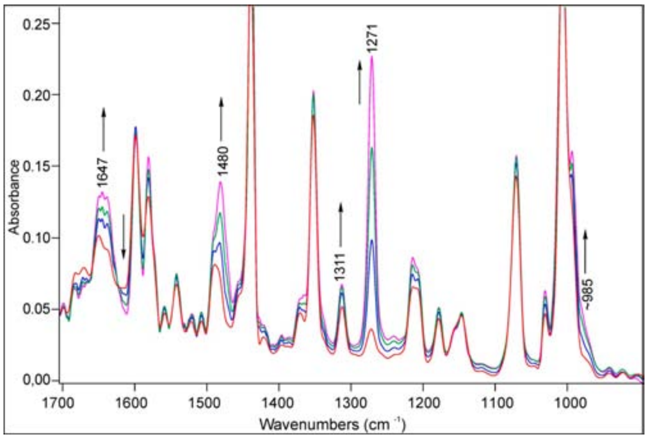

Figure 6. FTIR spectra of (Py)Co(TPP)(O_2) + NO system upon warming from 180 to 210 K.

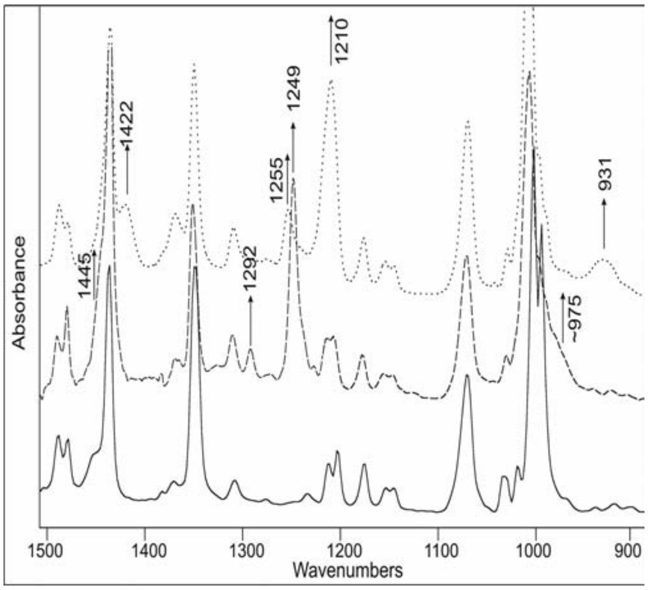

Figure 7. FTIR spectra at 210 K of (Py)Co(TPP) (solid line), (Py)Co(TPP)(η^1-$O^{15}NO_2$) (dashed), and (Py)Co(TPP)-(η^1-$^{18}O^{15}N^{18}O_2$) (dotted line). Some minor quantities of nitro complexes (Py)Co(TPP)($^{15}NO_2$) and (Py)Co(TPP)($^{15}N^{18}O_2$) are also present in the sample, manifesting themselves by the weak bands at 1292 and 1255 cm^{-1} representing the $\nu_s(^{15}NO_2)$ and $\nu_s(^{15}N^{18}O_2)$ of these species, correspondingly.

In these compounds the nitrate group is coordinated through one of the oxygen atoms in a monodentate fashion. The three IR-active stretching modes expected for this structure would be a low-frequency ν(O−N) band for the coordinated oxygen and two (symmetric and asymmetric) modes for the uncoordinated NO_2 fragment. Therefore, the bands in the vicinity of 1480 (m), 1270 (s), and 985 (w) cm^{-1} should be assigned to the vibrations that predominantly belong to $\nu_a(NO_2)$, $\nu_s(NO_2)$, and ν(O−N) stretching of the coordinated nitrato group.[26] The latter weak band is overlapped by the intense porphyrin band at 1000 cm^{-1} and is seen distinctly only for the species with both nitrogen and oxygen labels (Figure 7, dotted line).

The electronic absorption spectra of Co−porphyrins also undergo noticeable changes upon formation of both the six-coordinate dioxygen and nitrato complexes. Upon formation of the dioxygen complex (Py)Co(TPP)(O_2) the Q-band of Co(TPP) at 533 nm undergoes a red shift to 543 nm (Figure 2) and shifts farther to 549 nm (Figure S5, Supporting Information) upon formation of nitrato complex (Py)Co-(TPP)(η^1-ONO_2), indicating an increasing metal oxidation state.

The fate of thermally unstable six-coordinate nitrato complexes (Py)Co(Por)(η^1-ONO_2) upon warming depends on the experimental conditions. When nitric oxide was pumped out from the cryostat at 200 K and the layers were allowed to warm to toom temperature, the spectral changes reproduced in Figure 8 are observed. The bands of the coordinated nitrato group at 1480 and 1271 cm^{-1} disappear, and a new broad band overlapping with the porphyrin band at 1352 cm^{-1} grows in this range. As seen in Figure 8, the band at 1438 cm^{-1} also

Table 1. FTIR Frequencies of Coordinate Nitrato Group in Six-Coordinate Complexes (in parentheses are given the data for CoTTP derivatives)

compd	$\nu_a(NO_2)$ (m)	$\nu_s(NO_2)$ (s)	ν(O−N) (w)	ref
(Py)Co(TPP)(η^1-ONO_2)	1477 (1278)	1270 (1271)	~985 (~985)	this work
(Py)Co(TPP)(η^1-$O^{15}NO_2$)	~1447 (1448)	1249 (1248)	978 (977)	this work
(Py)Co(TPP)(η^1-$^{18}ON^{18}O_2$)	1455 (1456)	1245 (1245)	938 (937)	this work
(Py)Co(TPP)(η^1-$^{18}ON(^{18}O)O$)	1470 (1470)	1255 (1254)	946 (948)	this work
(Py)Co(TPP)(η^1-$^{18}O^{15}N^{18}O_2$)	1422 (1423)	1210 (1211)	931 (932)	this work
(NH_3)Co(TPP)(η^1-ONO_2)	1484 (1485)	1270 (1269)	~983 (983)	9
(NH_3)Co(TPP)(η^1-$O^{15}NO_2$)	1459 (1460)	1248 (1247)	~970 (970)	9
(NH_3)Co(TPP)(η^1-$^{18}ON^{18}O_2$)	1456 (1460)	1244 (1243)	942 (935)	9
(NH_3)Co(TPP)(η^1-$^{18}ON(^{18}O)O$)	1465(1470)	1252(1254)	953(955)	9
(NH_3)Co(TPP)(η^1-$^{18}O^{15}N(^{18}O)O$)	1437(1438)	1228(1229)	946(946)	9
(NH_3)Fe(TPP)(η^1-ONO_2)	1499(1496)	1268(1268)	938(936)	7
(NH_3)Fe(TPP)(η^1-$^{18}ON(^{18}O)O$)	1481(1482)	1252(1253)	913(914)	7
(NH_3)Fe(TPP) η^1-$O^{15}NO_2$)	1472(1469)	1249(1249)	925(925)	7

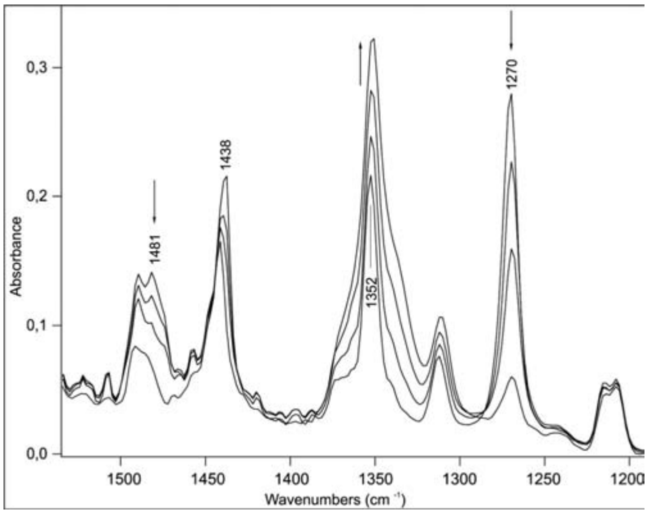

Figure 8. FTIR spectral changes demonstrating the formation of $[Co(TPP)(Py)_2]^+NO_3^-$ ionic couple upon warming (Py)Co(TPP)-(η^1-ONO_2) from 210 to room temperature.

decreases in intensity, since it consists of the overlapping bands of the porphyrin itself, and an intense Py band is occasionally disposed in the same spectral range. In the course of warming, this excess Py passes from the layer to the gas phase, diminishing the intensity of this band. The band in the vicinity of 1350 cm^{-1} has its isotopic analogs in the experiments with ^{15}N- (Figure 9) and ^{18}O-containing species and unambiguously should be assigned to the degenerate asymmetric stretching mode ν_3 of the nitrate anion.[26] Sustaining this interpretation, a weak isotopically sensitive band also grows in the vicinity of 830 cm^{-1}, where the out-of-plane deformation mode ν_2 of NO_3^- anion is disposed.[26]

The results obtained clearly indicate that six-coordinate nitrato complexes of Co−porphyrins decompose at room temperature to the nitrate anion and amino complexes of Co(III)−porphyrins. In contrast to the Co(II) species, the six-coordinate complexes of Co(III)−porphyrins with nitrogen donor ligands are much more stable.[27] Since in our experiments in the course of warming to room temperature there is excess Py in the layer (see above), the formation of bis-ligated $Co(III)(Por)(Py)_2$ instead of monoligated Co(III)(Por)(Py) species should be favorable (Scheme 4). The species eventually formed in the course of the NOD reaction is fairly stable, and high-vacuum pumping upon warming the system to 350 K does not reveal noticeable spectral changes. The result obtained in this work is similar to that for heme-containing globins[4] and modeling iron−porphyrin systems,[7] in which the NOD reaction results in the formation of nitrate anion and oxidized hemes. It is worthwhile to note, however, that just because the cobalt system is able to trap a peroxynitrite intermediate does not prove that the same intermediate has a viable lifetime or the same chemistry as the iron analog.

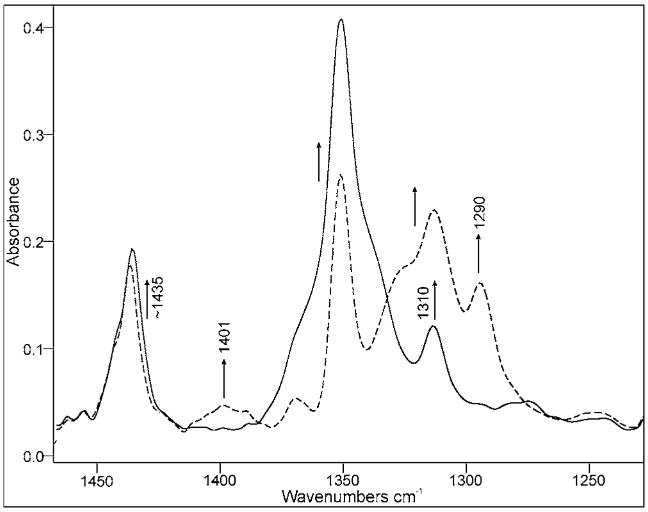

Figure 9. FTIR spectra of the products of NOD reaction at room temperature: $Co^{III}(TPP)(Py)_2NO_3^-$ (solid line) and $Co^{III}(TPP)$-$(Py)_2{}^{15}NO_3^-$ (dashed line). The samples contain some minor quantities of $(Py)Co(Por)(NO_2)$ and $(Py)Co(Por)(^{15}NO_2)$, correspondingly.

Formation of the Nitro Complexes $(Py)Co(Por)(NO_2)$ upon Warming Nitrato Complexes (Py)Co(TPP)(η^1-ONO_2) in NO Atmosphere. It was noticed that, if after formation of the six-coordinate nitrato complexes the gas-phase NO was not pumped out, together with formation of ionic couple mentioned above, some increase of the quantity of nitro−pyridine complexes $(Py)Co(Por)(NO_2)$ was observed. Therefore, after formation of the nitrato complexes and pumping at 200 K, a new higher portion of NO was added into the cryostat and warming the system to room temperature was spectrally monitored. As is seen from Figure 10, this procedure leads to the disappearance of the nitrate bands at 1481, 1270, and ~985 cm^{-1}, and those of previously formed

Scheme 4

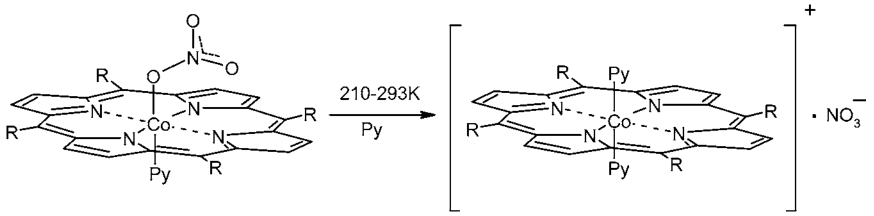

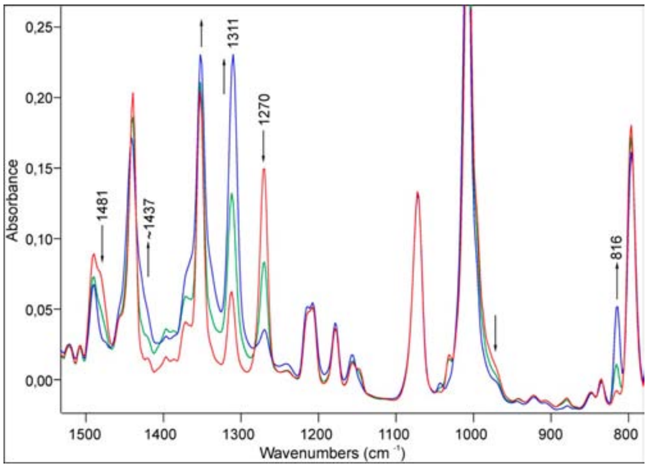

Figure 10. FTIR spectral changes upon warming layers containing six-coordinate nitrato complexes (Py)Co(TPP) (η^1-ONO_2) from 210 to room temperature in the presence of 5 Torr of NO. The final spectrum corresponds to the sample containing mostly (Py)Co(Por)(NO_2).

nitro complex at ~1437, 1311, and 816 cm^{-1} sharply increase their intensities. Some minor quantity of the ionic species is also formed during this process, as is evident from the growth of the band in 1350 cm^{-1} range. Upon this reaction the Q-band of nitrato complex undergoes a minor blue shift with its maximum disposed at 547 nm (Supporting Information, Figure S6).

These data indicate that formally the oxo-transfer reaction from the coordinating nitrato group to nitric oxide takes place, resulting in formation of the nitro complexes (eq 7).

$$\begin{aligned}&(Py)Co(TPP)(\eta^1\text{-}ONO_2) + NO\\&\quad \rightarrow (Py)Co(TPP)(NO_2) + NO_2 \qquad (7)\end{aligned}$$

Three different pathways may be considered in evaluating the mechanism of this reaction:

The first scenario suggests that NO through its nitrogen attacks coordinated oxygen (marked by asterisks) of the nitrate group with simultaneous β-bond cleavage (eq 8). The nitrito complex thus formed will quickly isomerize to the nitro form.[28]

$$\begin{aligned}&(Py)Co^{III}(TPP)(O^*NO_2) + NO\\&\quad \rightarrow (Py)Co^{III}(TPP)(\eta^1\text{-}O^*NO) + NO_2\\&\quad \rightarrow (Py)Co^{III}(TPP)(NO_2^*) + NO_2 \qquad (8)\end{aligned}$$

The second scenario involves oxygen atom abstraction from the coordinated nitrato ligand by excess NO to give nitrito species with the subsequent nitrito−nitro isomerization (eq 9).

Scheme 5

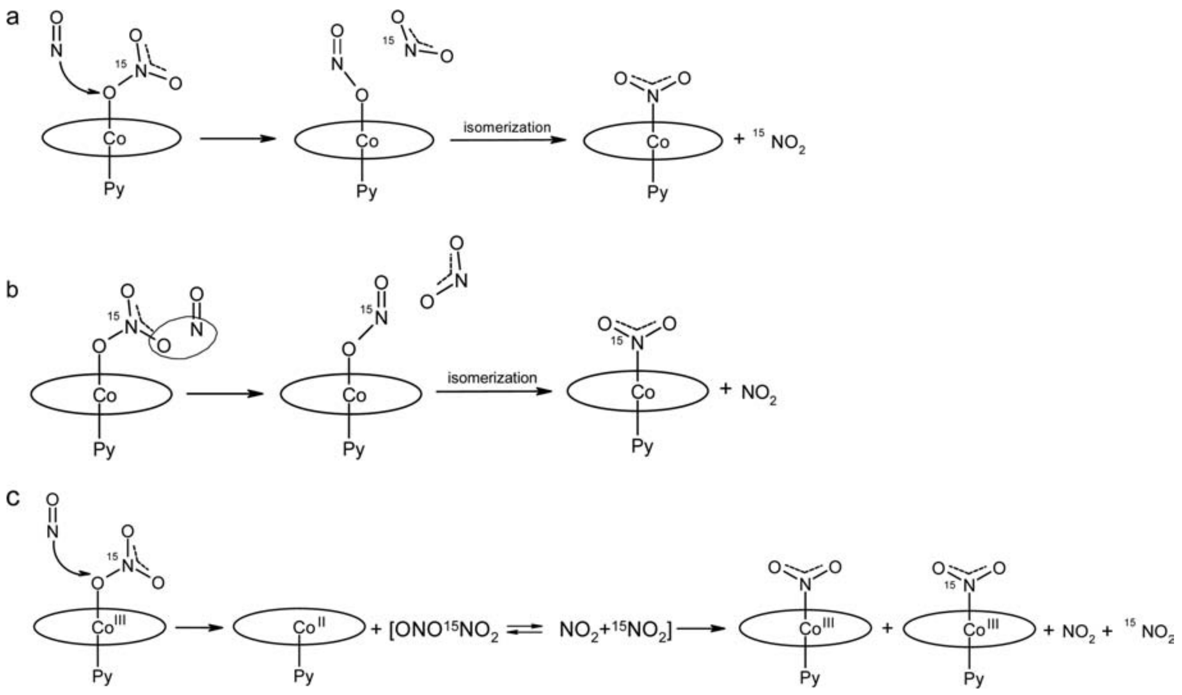

$$\begin{aligned}&(Py)Co^{III}(TPP)(\eta^1\text{-}ONO_2{*}) + NO\\ &\quad\rightarrow (Py)Co^{III}(TPP)(\eta^1\text{-}ONO) + NO_2{*}\\ &\quad\rightarrow (Py)Co^{III}(TPP)(NO_2) + NO_2{*} \qquad (9)\end{aligned}$$

The third scenario would be initiated by NO attack to the coordinated oxygen of the nitrate and dissociation of nitroso nitrate to give $(Py)Co^{II}(TPP)$, which is then rapidly oxidized to $(Py)Co^{III}(TPP)(NO_2)$ by reaction with the NO_2 resulting from decomposition of thermally unstable $ONONO_2$ (eqs 10−12).

$$\begin{aligned}&(Py)Co^{III}(TPP)(\eta^1\text{-}O{*}NO_2) + NO\\ &\quad\rightarrow (Py)Co^{II}(TPP) + ONO{*}NO_2 \qquad (10)\end{aligned}$$

$$ONONO_2 \rightleftharpoons 2NO_2 \qquad (11)$$

$$(Py)Co^{II}(TPP) + NO_2 \rightarrow (Py)Co^{III}(TPP)(NO_2) \qquad (12)$$

IR measurements with isotopically labeled NO were used to lend insight into differentiating these pathways. For example, for reaction of $(Py)Co^{III}(TPP)(\eta^1\text{-}O^{15}NO_2)$ with excess NO, different products are predicted according to the three scenarios. The first scenario (Scheme 5a) should give $(Py)Co(TPP)(NO_2)$, the second scenario (Scheme 5b) should give $(Py)Co(TPP)(^{15}NO_2)$, and the third scenario (Scheme 5c) should give a mixture of $(Py)Co(TPP)(NO_2)$ and $(Py)Co(TPP)(^{15}NO_2)$. The results were as follows: Figure 11 displays the FTIR spectral changes observed when excess NO was added to $(Py)Co^{III}(TPP)(\eta^1\text{-}O^{15}NO_2)$ and then the layer was slowly warmed from 210 K to room temperature. As seen, the intensity of the $\nu_s(NO_2)$ stretching band of $(Py)Co^{III}(TPP)(\eta^1\text{-}O^{15}NO_2)$ at 1249 cm^{-1} gradually decreases and two bands at 1310 and 1289 cm^{-1} increase in intensity. These bands certainly belong to $\nu_s(NO_2)$ and $\nu_s(^{15}NO_2)$ of the corresponding $(Py)Co(TPP)(NO_2)$ and $(Py)Co(TPP)(^{15}NO_2)$ complexes. Sustaining this assignment is the observation that the bands at ∼1430 (1400) and 816 (808) cm^{-1} (not shown) belonging to $\nu_{as}(NO_2)$ $[(\nu_{as}(^{15}NO_2)]$ and $\delta(NO_2)$ $[(\delta(^{15}NO_2)]$ grow with correlating intensities. During warming some minor quantity of $^{15}NO_3^-$ is also released, forming cationic $Co^{III}(TPP)(Py)_2$ complex, as evidenced by the growth of the broad weak band in the vicinity of 1320 cm^{-1} (see above). Hence, both six-coordinate nitro complexes with labeled and unlabeled nitrogen dioxide are formed during the reaction. This result is consistent with the third scenario considered above. This mechanism predicts the formation of two NO_2 molecules with natural and labeled nitrogen upon decomposition of nitroso nitrate $ONO^{15}NO_2 = NO_2 + {}^{15}NO_2$, and the formation of equal quantities of unlabeled and labeled nitro complexes $(Py)Co(TPP)(NO_2)$ and $(Py)Co(TPP)(^{15}NO_2)$ should be expected (Scheme 5c). However, in the presence of NO excess, $^{15}NO_2$ must be the subject of isotope scrambling (see Figure S3, Supporting Information), resulting in additional quantities of unlabeled NO_2. This in turn will enhance the relative quantity of $(Py)Co(TPP)(NO_2)$, so the higher intensity of the 1310 cm^{-1} band with regard to that at 1289 cm^{-1} is quite logical. It should be added that the higher intensity of the former band is partly connected also with the overlapping with the $\nu_3(E)$ band of the $^{15}NO_3^-$ anion.

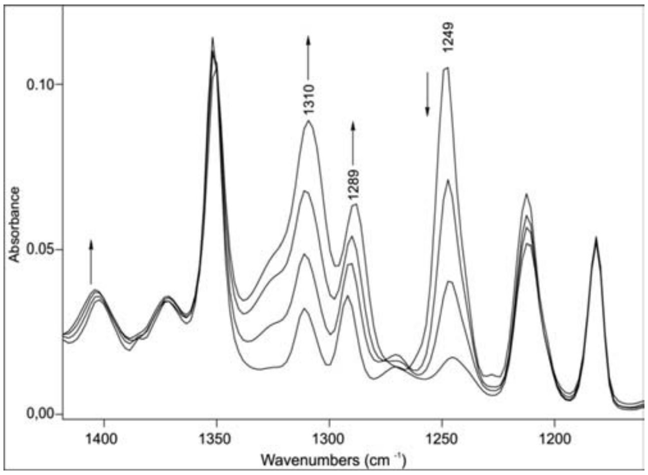

Figure 11. FTIR spectral changes upon supplying NO (5 Torr) to the layer containing mostly $(Py)Co^{III}(TPP)(\eta^1\text{-}O^{15}NO_2)$ and slow warming from 210 K to room temperature.

The closely related reaction was previously observed in the course of low-temperature interaction of NO with nitrato−nitrosyl complexes of iron−porphyrins $(NO)Fe(Por)(\eta^1\text{-}ONO_2)$,[24b] leading to the formation of nitro−nitrosyl complexes $(NO)Fe(Por)(NO_2)$.[20] The isotope labeling experiments performed in that study also give preference to the mechanism suggested here. In that case, however, the reaction proceeds at lower temperatures, at which the N_xO_y species formed in the course of the reaction still are stable and present in the spectra, complicating their assignment. Under the conditions of this experiment, the N_xO_y species is already dissociate, significantly facilitating the interpretation of the spectra. In effect, the third scenario represents a reductive nitrosylation reaction,[29] in which the coordinated anion is nitrosylated concomitant with the reduction of the metal center [in this case the reduced metal species is $(Py)Co^{II}(Por)$].

■ CONCLUSIONS

As shown by FTIR and UV−visible spectroscopy NO reacts at low temperatures with layered oxy−coboglobin model compounds, $(Py)Co(Por)(O_2)$, giving the six-coordinate nitrato complexes $(Py)Co(Por)(^1\eta\text{-}ONO_2)$ via initial formation of the six-coordinate peroxynitrite complex $(Py)Co(Por)(\eta^1\text{-}OONO)$. Simultaneously, due to weak binding some O_2 is released from the parent adduct, leading to NO autoxidation and formation of the N_xO_y species in the layer. As a result, together with nitrato complexes, some quantities of six-coordinate nitro and nitrosyl complexes with *trans*-pyridine ligand are also formed. The relative quantities of these species depend on the experimental conditions, and the yield of nitro and nitrosyl complexes is minimized when higher Py quantities are used in the experiments. The presence of N_xO_y species gave an opportunity to demonstrate the formation of the caged radical pair after homolytic disruption of the peroxynitrite O−O bond. The six-coordinate nitrato complexes, $(Py)Co(Por)(\eta^1\text{-}ONO_2)$, are not thermally stable, and the nature of products formed upon warming depends on the experimental conditions. In the absence of NO atmosphere, the nitrate is released as an anion to form cationic $[Co(Por)(Py)_2]^+$ and outer-sphere NO_3^-. In the presence of NO, however, the main part of the nitrato complexes is transferred to the six-coordinate nitro complexes $(Py)Co(Por)(NO_2)$, formally indicating the oxo-transfer reactivity of the six-coordinate nitrato complexes regarding NO. By using differently labeled nitrogen oxide, the plausible mechanism of this reaction was suggested.

■ ASSOCIATED CONTENT

Supporting Information

Figure S1 representing FTIR spectral changes accompanying the formation of (Py)Co(Por). Figure S2 representing FTIR spectra of (Py)Co(TPP)(O_2) and (Py-d_5)Co(TPP)(O_2) in the range of $\nu(O_2)$ stretching. Figure S3 representing the FTIR spectra demonstrating isotope scrambling of *asym*-$^{15}N_2O_3$ in a NO atmosphere. Figure S4 representing FTIR spectra in the 1100−750 cm^{-1} range evidencing formation of the caged radical pair after O−O bond disruption in the peroxynitrite moiety. Figure S5 demonstrating visible spectra of (Py)Co(TPP)(O_2) and (Py)Co(TPP)(η^1-ONO$_2$). Figure S6 demonstrating visible spectra of (Py)Co(TPP)(η^1-ONO$_2$) and (Py)Co(TPP)(NO_2). Table S1 representing experimental and computational vibrational frequencies for differently labeled peroxynitrite group in (Py)Co(TPP)(OONO). This material is available free of charge via the Internet at http://pubs.acs.org.

■ AUTHOR INFORMATION

Corresponding Author

*E-mail: kurto@netsys.am.

Notes

The authors declare no competing financial interest.

■ ACKNOWLEDGMENTS

This work was supported by the State Committee of Science RA (Grant #13-1D033).

■ REFERENCES

(1) (a) Tonzetich, Z. J.; McQuade, L. E.; Lippard, S. J. *Inorg. Chem.* **2010**, *49*, 6338−6348. (b) Ignarro, L. *Nitric Oxide: Biology and Pathobiology*; Academic Press: San Diego, CA, 2000.

(2) Ford, P. C.; Lorkovic, I. M. *Chem. Rev.* **2002**, *102*, 993−1017.

(3) (a) Pacher, P.; Beckman, J. S.; Liaudet, L. *Physiol. Rev.* **2007**, *87*, 315−324. (b) Nathan, C.; Shiloh, M. U. *Proc. Natl. Acad. Sci. U. S. A.* **2000**, *97*, 8841−8848. (c) Herold, S.; Koppenol, W. H. *Coord. Chem. Rev.* **2005**, *249*, 499−506. (d) Gardner, P. R.; Martin, L. A.; Hall, D.; Gardner, A. M. *Free Radical Biol. Med.* **2001**, *31*, 191−204. (e) Groves, J. T. *Curr. Opin. Chem. Biol.* **1999**, *3*, 226−235.

(4) (a) Su, J.; Groves, J. T. *Inorg. Chem.* **2010**, *49*, 6317−6329. (b) Schopfer, M. P.; Wang, J.; Karlin, K. D. *Inorg. Chem.* **2010**, *49*, 6267−6282. (c) Su, J.; Groves, J. T. *J. Am. Chem. Soc.* **2009**, *131*, 12979−12988. (d) Lee, J. B.; Hunt, J. A.; Groves, J. T. *J. Am. Chem. Soc.* **1998**, *120*, 7493−7501. (e) Moënne-Loccoz, P. *Nat. Prod. Rep.* **2007**, *24*, 610−620. (f) Schopfer, M. P.; Mondal, B.; Lee, D.-H.; Sarjeant, A. A. N.; Karlin, K. D. *J. Am. Chem. Soc.* **2009**, *131*, 11304−11305.

(5) (a) Herold, S. *FEBS Lett.* **1998**, *439*, 85−88. (b) Herold, S.; Exner, M.; Nauser, T. *Biochemistry* **2001**, *40*, 3385−3395. (c) Olson, J. S.; Folley, E. W.; Rogge, C.; Tsai, A.-L.; Dohle, M. L.; Lemon, D. D. *Free Radical Biol. Med.* **2004**, *36*, 685−697.

(6) Goldstein, S.; Merenyi, G.; Samuni, A. *J. Am. Chem. Soc.* **2004**, *126*, 15694−15701. Yukl, E. T.; de Vries, S.; Moenne-Loccoz, P. *J. Am. Chem. Soc.* **2009**, *131*, 7234−7235.

(7) Kurtikyan, T. S.; Ford, P. C. *Chem. Commun.* **2010**, *46*, 8570−8572.

(8) Koebke, K. J.; Pauly, D. J.; Lerner, L.; Liu, X.; Pacheco, A. A. *Inorg. Chem.* **2013**, *52*, 7623−7632.

(9) Kurtikyan, T. S.; Eksuzyan, Sh. R.; Hayrapetyan, V. A.; Martirosyan, G. G.; Hovhannisyan, G. S.; Goodwin, J. A. *J. Am. Chem. Soc.* **2012**, *134*, 13861−13870.

(10) Roat-Malone, R. M. *Bioinorganic Chemistry: A Short Course*; John Wiley & Sons Inc.: New York, 2007, 501 pp.

(11) (a) Kurtikyan, T. S.; Gasparyan, A. V.; Martirosyan, G. G.; Zhamkochyan, G. A. *J. Appl. Spectrosc.* **1995**, *62*, 62−65. (b) Kurtikyan, T. S.; Ford, P. C. *Coord. Chem. Rev.* **2008**, *252*, 1486−1496.

(12) (a) Epstein, L. M.; Straub, D. K.; Maricondi, C. *Inorg. Chem.* **1967**, *6*, 1720−1722. (b) Bhatti, W.; Bhatti, M.; Imbler, P.; Lee, A.; Lorenzen, B. *J. Pharm. Sci.* **1972**, *61*, 307−309.

(13) (a) Walker, F. A. *J. Am. Chem. Soc.* **1973**, *95*, 1150−1153. (b) Walker, F. A. *J. Am. Chem. Soc.* **1973**, *95*, 1154−1159.

(14) (a) Kincaid, J. R.; Proniewicz, L. M.; Bajdor, K.; Bruha, A.; Nakamoto, K. *J. Am. Chem. Soc.* **1985**, *107*, 6775−6781. (b) Nakamoto, K. *Coord. Chem,.Rev.* **1990**, *100*, 363−402. (c) Proniewicz, L. M.; Golus, J.; Majcherczyk, H.; Bajdor, K.; Kincaid, J. R. *J. Chem. Phys.* **1994**, *98*, 12856−12860. (d) Proniewicz, L. M.; Nakamoto, K.; Kincaid, J. R. *J. Am. Chem. Soc.* **1988**, *110*, 4541−4545.

(15) Kozuka, M.; Nakamoto, K. *J. Am. Chem. Soc.* **1981**, *103*, 2162−2168.

(16) Kurtikyan, T. S.; Martirosyan, G. G.; Akopyan, M. E. *Kinet. Catal.* **2001**, *42*, 281−288.

(17) (a) Collman, J. P.; Berg, K. E.; Sunderland, C. J.; Aukauloo, A.; Vance, M. A.; Solomon, E. I. *Inorg. Chem.* **2002**, *41*, 6583−6596. (b) Kurtikyan, T. S.; Martirosyan, G. G.; Gasparyan, A. V.; Akopyan, M. E.; Zhamkochyan, G. A. *J. Appl. Spectrosc.* **1990**, *53*, 728−734.

(18) (a) Varetti, E. L.; Pimentel, G. C. *J. Chem. Phys.* **1971**, *55*, 3813−3821. (b) Lee, C.-I.; Lee, Y.-P.; Wang, X.; Qin, Q.-Z. *J. Chem. Phys.* **1998**, *109*, 10446−10455.

(19) (a) Hisatsune, I. C.; Devlin, J. P.; Wada, Y. *J. Chem. Phys.* **1960**, *30*, 714−719. (b) Fateley, W. G.; Bent, H. A.; Crawford, B. *J. Chem. Phys.* **1959**, *31*, 204−217.

(20) Kurtikyan, T. S.; Gulyan, G. M.; Martirosyan, G. G.; Lim, M. D.; Ford, P. C. *J. Am. Chem. Soc.* **2005**, *127*, 6216−6224.

(21) (a) Gershinovitz, H.; Eyring, H. *J. Am. Chem. Soc.* **1935**, *57*, 985−891. (b) Beckers, H.; Zeng, X.; Willner, H. *Chem.—Eur. J.* **2010**, *16*, 1506−1520. (c) Jacox, M.; Thompson, W. E. *J. Chem. Phys.* **2008**, *129*, 204306/1−15. (d) Galliker, B.; Kissner, R.; Nauser, T.; Koppenol, W. H. *Chem.—Eur. J.* **2009**, *15*, 6161−6168. (e) Gadzhiev, O. B.; Ignatov, S. K.; Razuvaev, A. G.; Masunov, A. E. *J. Phys. Chem.* **2009**, *113*, 9092−2101.

(22) (a) Kurtikyan, T. S.; Markaryan, E. R.; Mardyukov, A. N; Goodwin, J. A. *Inorg. Chem.* **2007**, *46*, 1526−1528. (b) Stepanyan, T. G.; Akopyan, M. E.; Kurtikyan, T. S. *Russ. J. Coordin. Chem.* **2000**, *26*, 425−428.

(23) Thyagarajan, S.; Incarvito, C. D.; Rheingold, A. L.; Theopold, K. H. *Inorg. Chim. Acta* **2003**, *345*, 333−339.

(24) (a) Gulyan, G. M.; Kurtikyan, T. S.; Ford, P. C. *Inorg. Chem.* **2008**, *47*, 787−789. (b) Kurtikyan, T. S.; Martirosyan, G. G.; Hakobyan, M. E.; Ford, P. C. *Chem. Commun.* **2003**, 1706−1707.

(25) Wyllie, G. R. A.; Munro, O. Q.; Schulz, Ch. E.; Scheidt, W. R. *Polyhedron.* **2007**, *26*, 4664−6472.

(26) Nakamoto, K. *Infrared and Raman Spectra of Inorganic and Coordination Compounds*, 3rd ed.; Wiley: New York, 1978; pp 244−247.

(27) (a) Scheidt, W. R.; Cunningham, J. A.; Hoard, L. G. *J. Am. Chem. Soc.* **1973**, *95*, 8289−8294. (b) Sugimoto, H.; Ueda, N.; Mori, M. *Bull. Chem. Soc. Jpn.* **1981**, *54*, 3425−3432.

(28) Seki, H.; Okada, K.; Iimura, Y.; Hoshino, M. *J. Phys. Chem. A* **1997**, *101*, 8174−8178.

(29) (a) Ford, P. C. *Inorg. Chem.* **2010**, *49*, 6226−6239. (b) Ford, P. C.; Fernandez, B. O.; Lim, M. D. *Chem. Rev.* **2005**, *105*, 2439−2455.